The Journal of Engineering

The 14th IET International Conference on AC and DC Power Transmission (ACDC 2018)

IET Journals
The Institution of Engineering and Technology

Application of UPFC to mitigate SSR in series-compensated wind farms

eISSN 2051-3305
Received on 23rd August 2018
Accepted on 19th September 2018
E-First on 18th December 2018
doi: 10.1049/joe.2018.8533
www.ietdl.org

Hongli Jiang[1] ✉, Ruihua Song[1], Ning Du[1], Peipeng Zhou[1], Bin Zheng[1], Yanan Han[1], Daye Yang[1]

[1]*State Key Laboratory of Power Grid Safety and Energy Conservation, China Electric Power Research Institute, Beijing, People's Republic of China*

✉ *E-mail: jianghongli1@epri.sgcc.com.cn*

Abstract: Flexible AC transmission systems have shown effective functionalities in promoting the system operation security and service reliability. Facing with series-compensated lines, subsynchronous resonance (SSR) may jeopardise the stability and mechanical facilities. The control strategy and simulation model of a unified power flow controller (UPFC) based on the *dq* decoupling control are deduced and constructed. Considering the impacts of grid-connected wind farms, SSR characteristics of the series-compensated system with UPFC are studied by the complex torque coefficient method and time-domain simulation. The results verify the capability of UPFC in attenuating SSR in wind farm integrations by utilising subsynchronous damping controllers coordinated with UPFC's main controllers. It also suggests that the shunt transformer−converter has a slight effect on SSR, whereas the series transformer−converter affects the system resonance characteristics significantly. Simulations are carried out on a typical power system model integrated with wind turbines.

1 Introduction

Series capacitor compensation is an effective and economical method to enhance transfer capability and transient stability of the long-distance transmission power systems. However, series compensation can also produce a significant adverse effect, well known as subsynchronous resonance (SSR) on the thermal turbine generator connected to the series-compensated power systems [1]. Meanwhile in order to reduce the overall consumption of fossil energy and carbon dioxide emissions, renewable resource of energy, especially wind power has been developing rapidly due to a series of factors, including cost decrease, technological progress, and policy support from government. The high penetration of grid-connected wind farms also presents stability problems [2, 3].

Flexible AC transmission systems (FACTS) have shown effective countermeasures in attenuating SSR. Based on practical and theoretical reports, many researchers attempted the application of various FACTS devices to mitigate SSR in series-compensated wind farms [4, 5]. As the most versatile of FACTS devices, unified power flow controller (UPFC) almost yields simultaneous control of all basic power system parameters, including voltage amplitude and angle, line impedance, and power flows. Considering these salient capabilities, it could be an effective approach to mitigate SSR in combination with series compensation systems. Considerable researches have been devoted to UPFC in SSR damping [6, 7].

This paper is organised as follows: (i) The basic configuration and its controller design of the researched system with a simple but representative models, control strategies, and analysis method have been illustrated. (ii) The impact of wind power for SSR and the effectiveness of subsynchronous damping controller (SSDC) by the complex torque coefficient method and time-domain simulation have been addressed. (iii) This paper has been summarised and the contribution of UPFC to the SSR mitigation in series-compensated wind farms has been assessed.

2 Methodology

This researched system starts with a typical wind-thermal-bundled power transmitted by the series-compensated system in North China, which is jeopardised by SSR. It is interesting to explore the feasibility to mitigate SSR with UPFC device.

The typically recomposed wind-thermal-bundled power system with a fixed 41.2% series compensation and UPFC devices is shown in Fig. 1. The sending side of the compensated transmission line includes several thermal power plants and wind power farms. Here, this paper focuses on the direct-drive permanent magnetic synchronous generator (PMSG) wind turbine generators (WTGs) based power farms, which is connected to the strong power systems with the ultra-high voltage AC/DC parallel transmission network in North China finally.

2.1 Simplified model of PMSG and wind farms

In Fig. 1, the wind farm is composed of a certain number of identical 1.5 MW direct-drive PMSG WTGs which is parallel-series-connected or series-parallel-connected inside the wind farms. Generally, a PMSG-based WTG consists of the following components: a wind turbine, a PMSG, a machine-side converter (MSC; a cascade circuit by a diode rectifier and a boost DC/DC converter), a DC link (a DC capacitor), a grid-side converter (GSC; a voltage source converter, abbreviated as VSC) and an LC filter (a filter composed of an inductor and a capacitor) [8].

For the simulation purposes, the following assumptions are set. (i) A wind farm adopts the same type of WTG and all generators operate under a similar condition. (ii) A 50 MW wind farm is transferred by a 110 kV line. (iii) Through a step-up transformer T1, the local 110 kV grid is connected to a 220 kV line. Then wind power is transmitted to the main power grid by a step-up transformer T2. The electricity from both the wind farm and the thermal power plant is transferred to the main grid by line 1 and line 2. (iv) As widely accepted that the grid-tied dynamics of a direct-drive PMSG mainly depends on its GSC, it is acceptable to neglect the dynamic process of the MSC and replace it by a controlled current source. This simplification is reasonable for the analysis without losing its generality.

2.2 Composition and simplified model of UPFC

As shown in Fig. 1, the assumed UPFC is composed of a static synchronous compensator (VSC 1) and a series static synchronous compensator (VSC 2) coupled together through a common DC link capacitor, which could provide bidirectional real power exchanges between the shunt part (VSC1) and series part (VSC2).

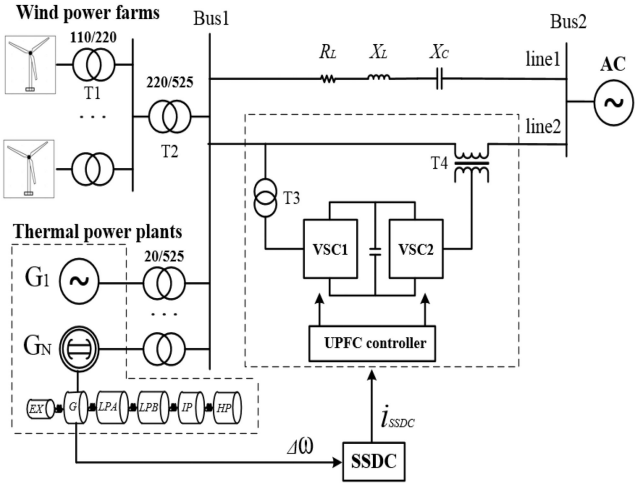

Fig. 1 *Typical wind-thermal-bundled model with UPFC and compensated line*

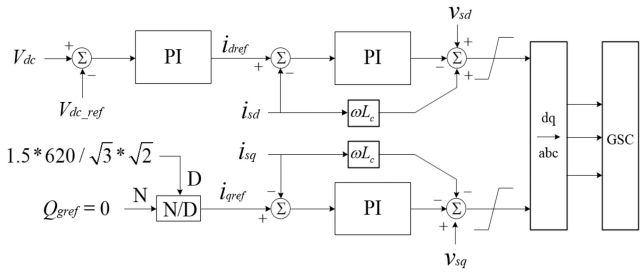

Fig. 2 *Control diagram of GSC*

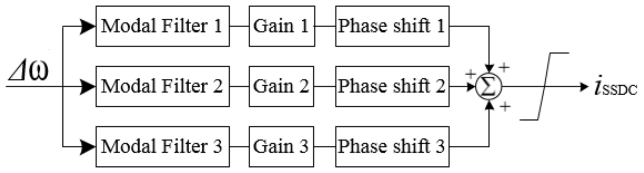

Fig. 3 *Structure of the narrow-band SSDC*

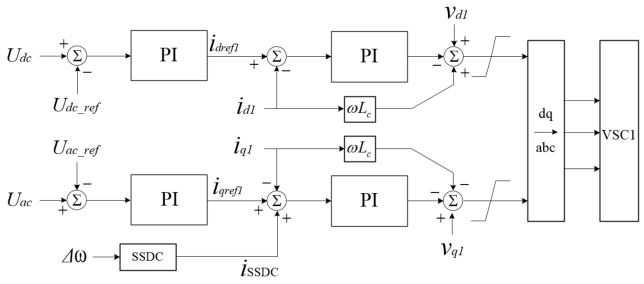

Fig. 4 *Control diagram of VSC1*

UPFC is a fairly flexible as well as powerful FACTS device. It is capable of controlling a couple of power system's basic parameters concurrently, such as voltage amplitude, phase angle, power flows, and line impedance. A variable set of objectives could be reached. In existing papers, diversified applications of UPFC in conjunction with different control strategies have been enumerated. The most common application of UPFC is to control its bus voltage by VSC1 (generating or absorbing reactive power with researched systems) and control the power flow on line 2 by VSC2 (injecting voltage of specific magnitude and phase). What is noteworthy is that both the series and shunt parts are able to operate in its connected power system independently [3, 6, 7].

In this paper, based on the main function of UPFC, as mentioned above, it is considered as an SSR countermeasure, and its main parameters are reported in Table 1.

All the mentioned VSC1 and VSC2 in UPFC and GSC in wind farms are controlled with a vector control strategy based on the *dq* decoupling reference frame. For VSC1, there are outer-loop controls for the DC and AC voltages at the shunt access point; for VSC2, there are outer-loop controls for active power and reactive power at the series access point; for GSC, the control objectives of its outer-loop are DC voltage and reactive power at the grid-connected point. All their inner-loop controls the *d*- and *q*-axis currents. Also, proportional-integral (PI) controllers are used in both outer- and inner-control loops (see Table 2).

Take GSC for example, and illustrate the symbols and parameters of its control unit in Table 2. Also, the control diagram of GSC is shown in Fig. 2.

Table 1 UPFC main parameters

Parameter	Value
rated power	2×80 MVA
rated DC link voltage	40 kV
frequency	50 Hz
X_{T3} (shunt)	0.1
X_{T4} (series)	0.1

Table 2 Symbols in control diagram of GSC

Symbols	Meanings
i_{sd}, i_{sq}	*d*- and *q*-axis component of GSC output current
v_{sd}, v_{sq}	*d*- and *q*-axis component of GSC output voltage
i_{sdref}, i_{sqref}	reference values for i_{sd}, i_{sq}
v_{gd}, v_{gq}	reference values for v_{sd}, v_{sq}
V_{dc}, V_{dcref}	DC voltage and its reference value
Q_{gref}	reference value of GSC output reactive power
ωL_c	decoupling gain

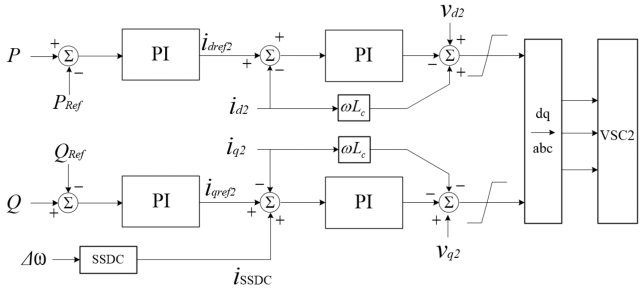

Fig. 5 *Control diagram of VSC2*

2.3 SSDC for SSR mitigation in UPFC controllers

In order to acquire the accurate SSR mode signal of torsional frequencies, an SSDC structure consisted of three parallel narrow band elements, as shown in Fig. 3, is used [9]. Each single element contains a modal filter, a gain, and a phase shift, all designed for a specific torsional frequency. The mechanism of the SSDC is to improve the damping of resonances. $\Delta\omega$ signifies the angular frequency difference of the generator. The output of different elements is superimposed as an additional current signal i_{SSDC}, which is clipped by the fixed upper and lower limits to keep the injected auxiliary current signal i_{SSDC} within the specified limits.

As mentioned above, VSC1 and VSC2 in UPFC are controlled based on the *dq* decoupling frame, the SSDC can be added to VSC1 and VSC2 separately or simultaneously to mitigate power oscillation. The modified controllers are demonstrated in Figs. 4 and 5. The tuned additional current signal i_{SSDC} can be superimposed in the *q*-axis current of the inner loop.

2.4 Complex torque coefficient method

As a kind of frequency-domain method, the complex torque coefficient method is widely used in the analysis of SSR of power systems. For a given SSR case, it is possible to divide its system

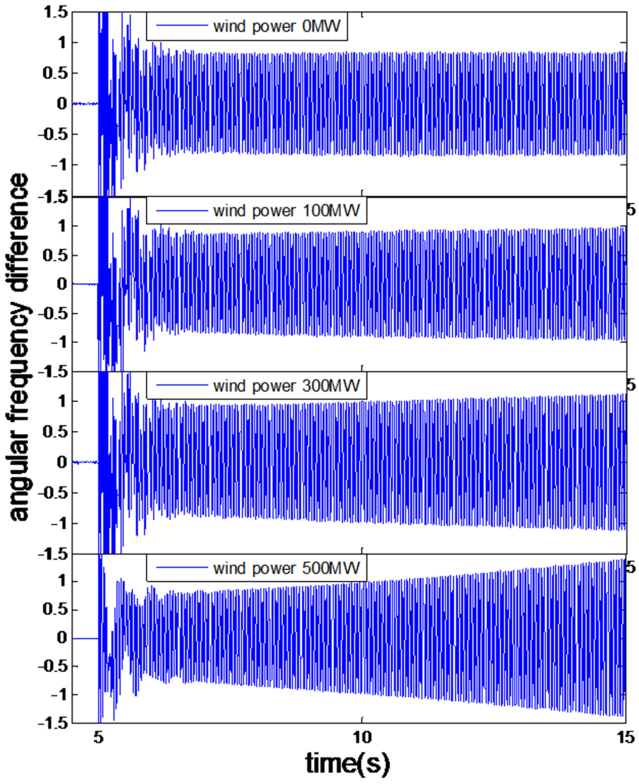

Fig. 6 *Angular frequency difference for different wind power*

state space into two parts: mechanical and electrical subsystems [10–13]. The mechanical subsystem is the shaft system of the thermal plants, which normally contains its multi-mass block model, while the electrical subsystem adopts the electromagnetic part and other external networks in the researched system. The mechanical and electrical subsystems are connected via the electromagnetic torque of the concerned unit and the rotor angle of the generator. Then the electrical complex torque coefficients and the mechanical complex torque coefficients could be calculated by solving the linearised state equation of the shaft system as follows:

$$\Delta Te = \left(De(\xi) + \frac{1}{j\xi}Ke(\xi)\right)\Delta\omega \tag{1}$$

where $Ke(\xi)$ and $De(\xi)$ are electrical spring and damping coefficients at frequency ξ. The complex torque coefficient analysis theory indicates that SSR would occur at the shaft system's certain natural frequency if the unit's positive mechanical damping was not enough to neutralise negative electrical damping. Thus, the complex torque coefficient approach realised by the time-domain simulation and test signal method is adopted in this paper to study the SSR damping characteristics in the series-compensated wind-thermal-bundled power transmitted system. From (1), we can obtain the electrical damping coefficient $De(\xi)$ as follows:

$$De(\xi) = \mathrm{Re}\left(\frac{\Delta Te(\xi)}{\Delta\omega(\xi)}\right) \tag{2}$$

3 Results of simulation and complex torque coefficients analyses

As shown in Fig. 1, the wattage rating of the thermal plant is 2 × 660 MW of the multi-mass block model with theoretical calculated torsional frequencies: 18.9 Hz (mode 1), 31.70 Hz (mode 2), and 57.75 Hz (mode 3), and mode 3 could be neglected in SSR analysis. The mechanical damping of thermal plants is considered and set at 0.07 pu. The single-phase transient fault took place at t = 5 s and lasted for 0.05 s. The fault point was set on bus1 in Fig. 1.

The installed wind power plant is of 500 MW, and the grid-connected wind power output varies from 0 to 500 MW. The simulation model of the analysis system based on power systems

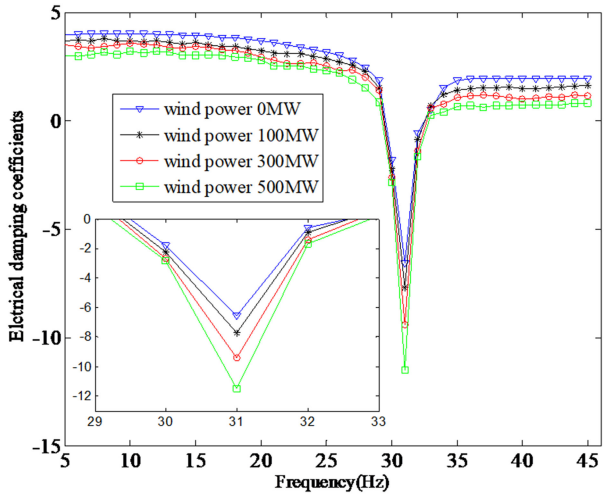

Fig. 7 *Electrical damping coefficients of different wind power output*

computer aided design/electromagnetic transients including DC (PSCAD/EMTDC) has been built. This paper considered the following four typical operation cases of the researched system.

- *Case1:* without UPFC and wind farms.
- *Case2:* with wind farms, adjust the wind power output in different values: 100, 300, 500 MW.
- *Case3:* with UPFC and 500MW wind power output
- *Case4:* apply SSDC for VSC1 and VSC2 separately and simultaneously.

3.1 SSR in series-compensated wind farms

Firstly, neglecting the impact of UPFC device, only the wind-thermal-bundled power is transmitted by line 2 without FACTS devices and line 1 with a fixed 41.2% series compensation. Based on the simplified PMSG wind farms, keep the thermal plants in rated output power and adjust the wind power output in different values: 0,100, 300, 500 MW. The contingency stimulating the SSR is a transient single-phase-to-ground fault in bus 1.

The angular frequency difference $\Delta\omega$ is separately obtained for each case and the time-domain representation is shown in Fig. 6. When there is no wind power, the waveform of $\Delta\omega$ is almost an equal amplitude oscillation. However, the more the wind power injects, the larger the magnitude of oscillation is. When the wind power is 500 MW, the waveform is divergent and the system is unstable. With the increase of the penetration of the grid-connected wind power, the resonance magnitude of SSR becomes larger. That is to say, the wind power injection aggravates the SSR problem.

Analysing the above cases by the complex torque coefficient method, the electrical damping coefficients are shown in Fig. 7. According to the complex torque coefficient analysis theory, if the positive mechanical damping was not enough to neutralise negative electrical damping at the shaft system's certain natural frequency; thus, the general damping coefficient would be negative and SSR would be stimulated.

As shown in Fig. 7, in cases investigated above, the electrical damping coefficients of researched thermal plant generators are remarkable negative values at its torsional natural frequency: 31.70 Hz (mode 2). With the increasing output of wind power, the negative electrical damping coefficient is magnified and the SSR problem is exacerbated, which is consistent with the conclusions of the time-domain simulation.

3.2 UPFC controllers for SSR mitigation with SSDC

In the following research, to maintain the occurrence of SSR and investigate UPFC capability in the mitigation of SSR, the wind farm output power is fixed to be 500 MW and the thermal plants are in rated output power.

To investigate the SSR mitigation effects by utilising SSDC with UPFC in this researched system, assume the following

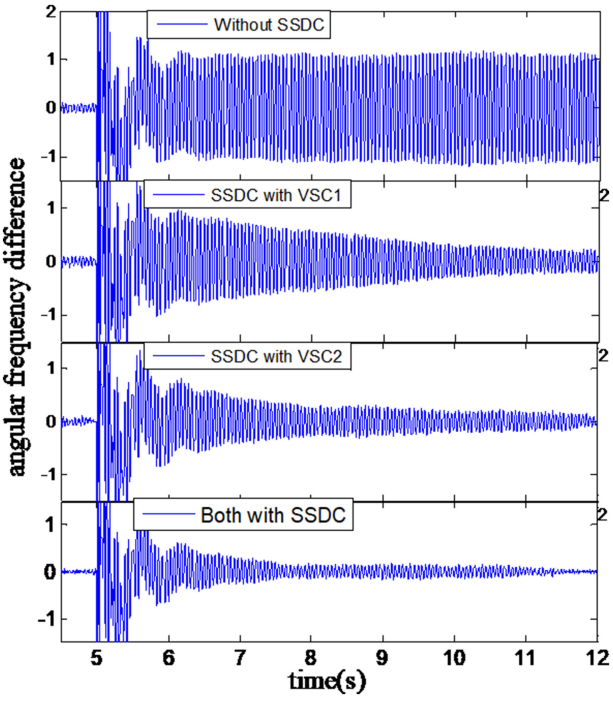

Fig. 8 *SSR mitigation using SSDC in UPFC*

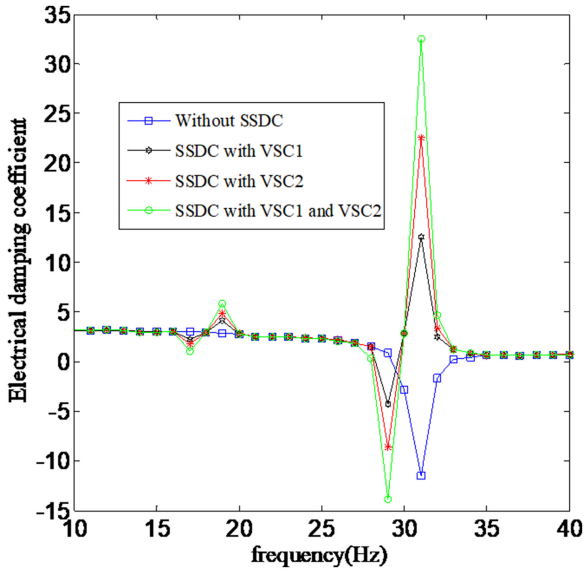

Fig. 9 *Electrical damping coefficients of operating conditions*

operating conditions: (i) apply UPFC without SSDC, (ii) apply SSDC for VSC1 separately, (iii) apply SSDC for VSC2 separately, and (iv) apply SSDC for VSC1 and VSC2 simultaneously.

Fig. 8 displays the oscillations of the generator angular frequency difference Δω. This figure reveals different SSR mitigation effects under various operating conditions. No matter whether SSDC is applied in VSC1 and VSC2 separately or simultaneously, the waveform is convergent and the researched system is stable. The main difference is the rapidity of the convergence. It is remarkable that the rate of decay decreases in utilising SSDC for VSC1 and VSC2 simultaneously, SSDC for VSC2 separately, and SSDC for VSC1 separately.

It is reasonable that the best damping performance occurs when SSDC operates for VSC1 and VSC2 simultaneously. Also, UPFC with SSDC on VSC2 shows a more superior damping effect than that on VSC1. The reason lies in the greater capacity of VSC2 in affecting the line's series impedance. As shown in Fig. 8, the best damping performance is achieved when SSDC is utilised for VSC1 and VSC2 simultaneously, so it is recommended to apply SSDC for both VSC1 and VSC2.

Analysing the influence of SSDC by the complex torque coefficient method, the electrical damping coefficients are shown in Fig. 9. Compared with the result of applying UPFC without SSDC, the negative electrical damping coefficient at torsional frequency is amended to the positive value significantly, which represents the mitigation effects of different operating conditions. The best situation appears in applying SSDC in both VSC1 and VSC2. Also, UPFC with SSDC on VSC2 gets a better revised value than that on VSC1, corresponded with the results of time-domain simulation.

4 Conclusion

Modal analysis is performed in a typical wind-thermal-bundled power system interconnected with a series-compensated transmission network. Based on PMSG WTGs, the wind power injection has a definite influence in SSR. As the occurrence of SSR is credible and deteriorated by the increase of the penetration of grid-connected wind power, wind power injection aggravates the instability of the researched system by amplifying its resonance magnitude of SSR.

The contribution of presented SSDC structures to mitigate SSR is confirmed in this paper. When both the SSDCs operate concurrently, UPFC presents the best performance in damping SSR. At the same time, UPFC with SSDC on VSC2 shows a more superior damping effect than that on VSC1 due to the stronger impact of the series inverter on the line power transfer by adjusting the line's series impedance. Moreover, in view of the best damping performance of resonances, the idea of utilising two SSD controllers coordinated with UPFC's main controllers was recommended.

All these conclusions are verified by both the complex torque coefficient method and time-domain simulation.

5 Acknowledgments

This work is supported by National Key R&D Program of China (2016YFB0900600), and Technology Projects of State Grid Corporation of China (52094017000W).

6 References

[1] IEEE Committee Report: 'Terms, definitions, and symbols for subsynchronous resonance oscillations', *IEEE Trans. Power Appar. Syst.*, 1985, **104**, (6), pp. 1326–1334

[2] Fan, L., Zhu, C., Miao, Z.: 'Modal analysis of a DFIG-based wind farm interfaced with a series compensated network', *IEEE Trans. Energy Convers.*, 2011, **4**, (26), pp. 1010–1020

[3] Sajjad, G., Farrokh, A., Daryoush, N.: 'Application of UPFC to enhancing oscillatory response of series-compensated wind farm integrations', *IEEE Trans. Smart Grid*, 2014, **5**, (4), pp. 1961–1968

[4] Bongiorno, M., Svensson, J., Angquist, L.: 'On control of static synchronous series compensator for SSR mitigation', *IEEE Trans. Power Electron.*, 2008, **2**, (23), pp. 735–743

[5] Varma, R.K., Auddy, S., Semsedini, Y.: 'Mitigation of subsynchronous resonance in a series-compensated wind farm using FACTS controllers', *IEEE Trans. Power Deliv.*, 2008, **3**, (23), pp. 1645–1654

[6] Padiyar, K.R., Prabhu, N.: 'Investigation of SSR characteristics of unified power flow controller', *Electr. Power Syst. Res.*, 2005, **2**, (74), pp. 211–221

[7] Wang, L., Li, H.W., Wu, C.T.: 'Stability analysis of an integrated offshore wind and seashore wave farm fed to a power grid using a unified power flow controller', *IEEE Trans. Power Syst.*, 2013, **3**, (28), pp. 2211–2221

[8] Liu, H., Xie, X., He, J., *et al.*: 'Subsynchronous interaction between direct-drive PMSG based wind farms and weak AC networks', *IEEE Trans. Power Syst.*, 2017, **32**, (6), pp. 4708–4720

[9] Rauhala, T., Järventausta, P.: 'On feasibility of SSDC to improve the effect of HVDC on subsynchronous damping on several lower range torsional oscillation modes'. IEEE PES General Meeting Conf., Minneapolis, Minnesota, America, July 2010, pp. 1–8

[10] Canay, I.M.: 'A novel approach to the torsional interaction and electrical damping of the synchronous machine, part I and part II', *IEEE Trans Power Appar. Syst.*, 1982, **101**, (10), pp. 3630–3647

[11] Zheng, X.: 'The complex torque coefficient approach's applicability analysis and its realization by time domain simulation', *Proc. the CESS*, 2000, **6**, (6), pp. 1–4

[12] Zhu, X., Sun, H., Wen, J., *et al.*: 'Improved complex torque coefficient method using CPCM for multi-machine system SSR analysis', *IEEE Trans. Power Syst.*, 2014, **32**, (5), pp. 2060–2068

[13] Feng, G., Yunsheng, W.: 'Analysis on damping characteristics of subsynchronous oscillation in Hulunbuir power plant'. IEEE PES APPEEC Conf., Hong Kong, China, December 2014, pp. 1–6